Effects of oxidant selection for atomic layer deposition on impurity removal and crystallinity of as-grown $Hf_{1-x}Zr_xO_2$ thin films

Haoming Che[1,a)], Takashi Onaya[1,2,a)], Atsushi Tamura[1], Masaki Ishii[3], Hiroshi Taka[3], and Koji Kita[1,a)]

[1]Graduate School of Frontier Sciences, Department of Advanced Materials Science, The University of Tokyo, 5-1-5 Kashiwanoha, Kashiwa, Chiba, Japan 277-8561
[2]Research Center for Materials Nanoarchitectonics (MANA), National Institute for Materials Science (NIMS), 1-1 Namiki, Tsukuba, Ibaraki, Japan 305-0044
[3]Tsukuba Laboratory, R&D Unit, Taiyo Nippon Sanso Corporation, 10 Okubo, Tsukuba, Ibaraki, Japan 300-2611

[a)] Electronic mail: 3316270435@edu.k.u-tokyo.ac.jp, onaya.takashi@nims.go.jp and kita@scio.t.u-tokyo.ac.jp

10-nm-thick $Hf_{1-x}Zr_xO_2$ (HZO) films were deposited on TiN by atomic layer deposition (ALD) at 250 °C using H_2O_2 or H_2O as an oxidant with various exposure time. X-ray diffraction results showed that all as-grown films exhibited an overlapping peak associated with the orthorhombic (O)/tetragonal (T)/cubic (C) phases, while no notable peaks of the monoclinic phase were observed. With extending oxidant exposure time, both H_2O_2- and H_2O-based films exhibited enhanced O/T/C phases peak area and reached saturation under sufficient oxidation. In the saturated region, the O/T/C phases peak area of H_2O_2-based films was ~30% higher than that of H_2O-based films. Carbon and nitrogen impurities were considered to remain in the films as residual precursor-ligand fragments due to incomplete reaction. With evaluation of impurity levels, both H_2O_2- and H_2O-based HZO films exhibited a trend that crystallinity increases as impurity concentration of carbon and nitrogen decreases. Moreover, H_2O_2-based films had carbon and nitrogen concentrations approximately one order of magnitude lower than those of H_2O-based films. These results

suggest that impurity removal during the oxidation step is a critical factor for enhancing the crystallization of as-grown HZO films.

I. INTRODUCTION

Since the first report of ferroelectricity in HfO_2-based thin film in 2011[1], it has gained considerable attention owing to its capacity to maintain robust ferroelectricity at nanometer-scale thicknesses, thereby enabling the development of highly integrated non-volatile memory devices[2]. Ferroelectricity of HfO_2-based thin films originates from the metastable orthorhombic (O) *Pca*2_1 phase[3-5], whose formation and stabilization can be controlled by an introduction of dopant such as Al[6], Si[7], Gd[8], and Zr[9,10]. Among them, Zr has attracted widespread interest because $Hf_{1-x}Zr_xO_2$ (HZO) offers a wide compositional window and enables low-temperature crystallization (<400 °C). Notably, $Hf_{0.5}Zr_{0.5}O_2$ was reported to exhibit the largest polarization[10,11]. For ferroelectric random access memory and related embedded applications, HZO films are expected to be integrated within back end of line process and three-dimensional (3D) structure devices, where the thermal budget is limited to 400 °C. This constraint makes the formation of high quality films with stable ferroelectricity challenging. Accordingly, these considerations motivate a detailed understanding of the low-temperature crystallization behavior of HZO films.

To precisely control the thickness and chemical composition of HZO thin films, atomic layer deposition (ALD) is regarded as an indispensable method. In ALD, film growth proceeds via alternating a self-limiting chemisorption of metal precursor and then a reaction with oxidant, separated by purge steps, which can form conformal films even

in 3D structures. Extensive studies have been conducted to understand how precursors influence HfO_2-based films' properties[12-14]. Meanwhile, oxidant plays a critical role in ligand removal in ALD[15,16], since residual ligands fragments from organic precursor can introduce impurities such as carbon[17] and nitrogen[18]. It is reported that carbon impurity can increase the crystallization temperature of ALD-grown HfO_2[19]and TiO_2[20] thin films. The mechanism has not been fully elucidated, but carbon may affect the migration rate of atoms[21], resulting in a higher thermal budget required for the completion of crystallization. The introduction of nitrogen has been proven to influence the crystallization of HfO_2 films[22]. Nitrogen was considered to reduce atoms migration rate and average coordination number[23], thereby increasing the crystallization temperature of HfO_2-based films. Thus, the design of oxidation process in ALD affects not only chemical purity but also crystallinity of HZO films. H_2O_2, with a high standard oxidation potential (1.78 V)[24], is expected to have stronger oxidizing ability than H_2O in ALD and to remove residual impurities more efficiently. HZO films grown by using H_2O_2 as an oxidant exhibited high polarization value ($2P_r$ ~55 $\mu C/cm^2$) even at low process temperature at 350 °C[25], suggesting the promising role of H_2O_2 for low-temperature process, but the origin of this enhancement was still not fully explored. Furthermore, previous studies indicated that partial crystallization in as-grown HZO films can play an important role in subsequent crystallization, because pre-existing nanocrystals formed during ALD process using O_2 plasma as an oxidant can act as nuclei that promote further crystallization during annealing even at temperature as low as 300 °C [26, 27]. This suggests that the crystallinity of as-grown HZO films should be directly examined in order to understand low-temperature crystallization behavior. Motivated by these considerations,

this paper systematically investigated the deposition of HZO thin films using H_2O_2 or H_2O as the ALD oxidant while varying oxidant exposure time, to explore the influence of oxidant selection on impurity concentration and crystallinity of as-grown HZO films, then examined the relationship between impurity concentration and crystallinity.

II. EXPERIMENTAL

HZO films with a thickness of 10 nm were deposited on TiN (15 nm)/Si substrates by ALD using a cocktail precursor composed of $Hf[N(C_2H_5)CH_3]_4$ (TEMAHf, 99.9999%; Kojundo Chemical Laboratory Co., Ltd.) and $Zr[N(C_2H_5)CH_3]_4$ (TEMAZr, 99.999%; Kojundo Chemical Laboratory Co., Ltd.) with a ratio of 1:1[26,27]. Deposition temperature was selected at 250 °C, which was within the ALD window of this TEMAHf/TEMAZr process as evaluated by growth rate of HZO films (data not shown). Either H_2O_2 or H_2O was employed as an ALD oxidant. In this study, the precursor and oxidants were introduced to the deposition chamber by pulses with a short duration of 0.65 s as illustrated in FIG. 1(a). This pulsed ALD sequence was adopted to provide a more reproducible reactant dose and to minimize partial-pressure drift that can occur during prolonged single-exposure dosing. Exposure time of oxidants were varied by changing the number of oxidant pulses, while the number of precursor pulses was fixed to 10 per cycle for all the depositions. H_2O_2/H_2O solution was vaporized using N_2 as a carrier gas, with Peroxidizer®, RASIRC Inc. The concentration of H_2O_2 was determined to be ~5% by a concentration monitor (product of Ebara Jitsugyo Technologies). The thickness of HZO films was measured by spectroscopic ellipsometry (SE). The growth per cycle (GPC) was extracted from the thickness and number of ALD cycles. The

crystallinity of as-grown HZO films was evaluated by X-ray diffraction (XRD). Furthermore, the impurity concentrations were measured by X-ray photoelectron spectroscopy (XPS) and secondary ion mass spectrometry (SIMS).

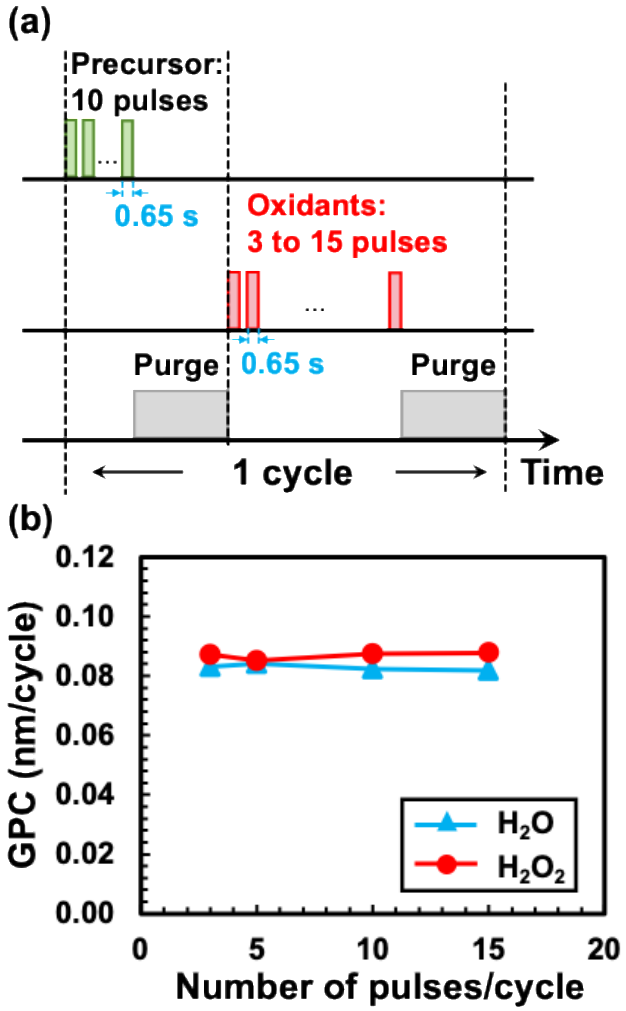

FIG. 1. (a) Illustration of ALD pulse sequence. (b) Variations in GPC of HZO films grown using either H_2O or H_2O_2 as an oxidant with various number of pulses per cycle.

III. RESULTS AND DISCUSSION

A. Deposition of HZO films

The Hf:Zr ratio of as-grown HZO films was estimated by XPS to be constant at around 0.55:0.45, which was not change regardless of oxidant gas. The GPC of H_2O- and H_2O_2-based HZO films were evaluated while systematically changing the number of oxidant pulses per cycle, as shown in FIG. 1(b). For both oxidants, GPC did not vary significantly according to the changes in number of oxidant pulses, but showed a stable GPC when using the same oxidant. This behavior is consistent with previous report that the GPC of ALD-grown HfO_2 thin films using H_2O_2 as an oxidant shows only a weak dependence on oxidant exposure time[28]. The average GPC obtained using H_2O_2 (~0.086 nm/cycle) was slightly higher than that obtained using H_2O (~0.082 nm/cycle), which indicates the differences in growth behavior for different oxidants. When compared with literature, those values are in a reasonable range, and our results is consistent with a report that H_2O_2 showed a higher growth rate than H_2O[29]. It was confirmed from these observations that the difference of crystallinity of two kinds of as-grown films can be examined without significant influence of growth rate variations.

B. Crystallinity of as-grown HZO films

XRD analysis was performed to evaluate the crystallinity of as-grown HZO films on TiN substrates using H_2O_2 or H_2O as an ALD oxidant, as shown in FIG. 2. For all the films, regardless of the employed oxidant or the number of oxidant pulses, a diffraction peak appeared at $2\theta \approx 30.7°$. This peak was assigned to a mixture of components from the (111) plane of the O phase, the (101) plane of the tetragonal (T) phase, and the (111) plane of the cubic (C) phase of HZO films. Furthermore, no notable peaks originating from the (−111) and (111) planes of the monoclinic (M) phase were observed at $2\theta \approx$ 28.5° and 31.6°, suggesting that the as-grown HZO films dominantly formed O/T/C

phase crystals with the detection limit of the present measurements. Because the peak positions of the O/T/C phases at 30.7° are very close, it is difficult to deconvolute this peak using our laboratory-based XRD with limited instrumental resolution. However, previous studies have reported that the peak position and peak area of O/T/C phases closely correlate with remanent polarization in HZO films[27,30,31]. Since the peak position is essentially unchanged among our samples, comparing the integrated O/T/C phases peak area provides a reasonable basis for assessing crystallinity trends.

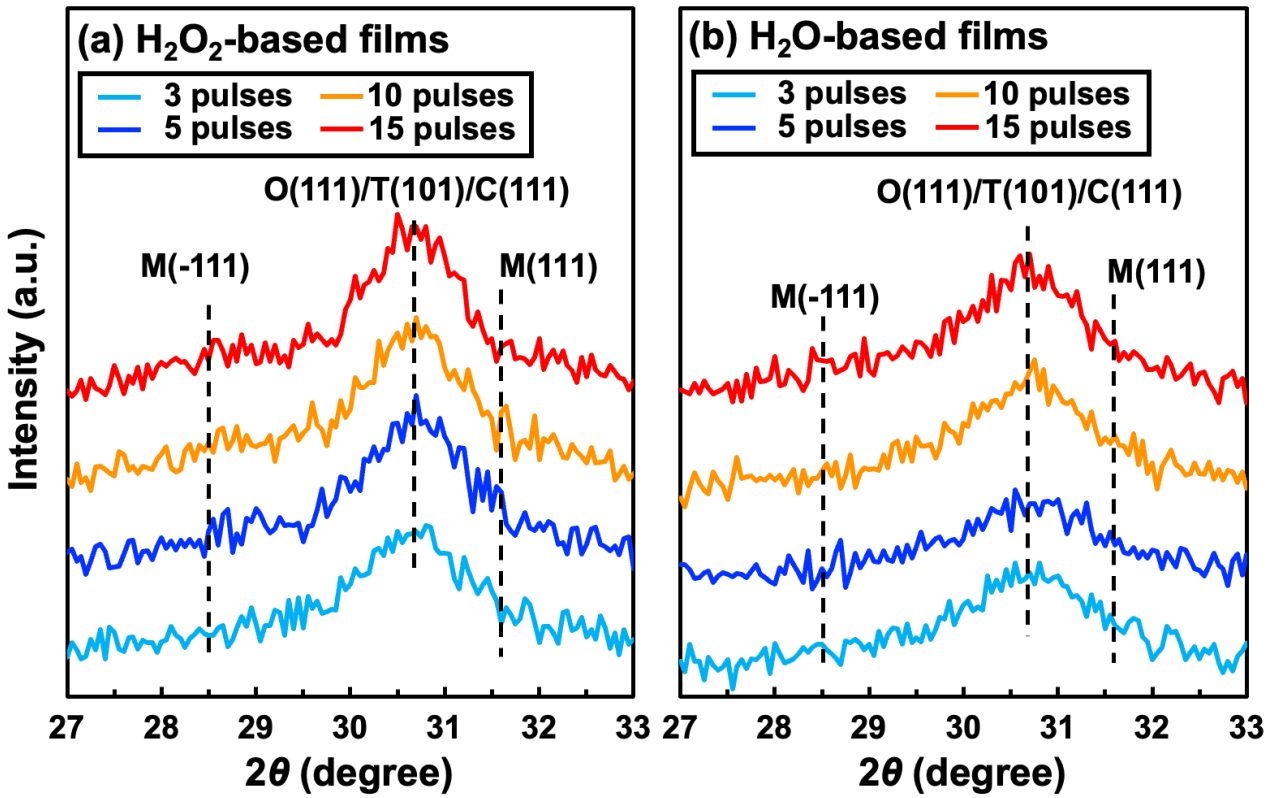

FIG. 2. XRD patterns of (a) H_2O_2 and (b) H_2O-based HZO films fabricated on TiN substrates using various numbers of oxidant pulses per cycle. Note that the scale of intensity in FIG. 2(a) and 2(b) is the same.

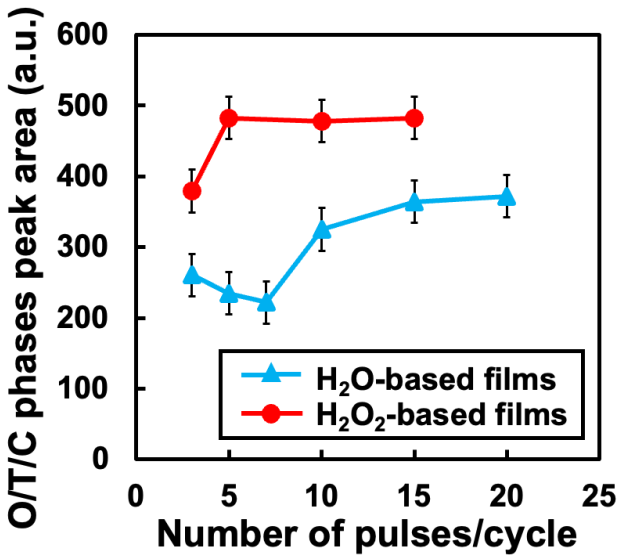

FIG. 3. O/T/C phases peak area of H_2O- and H_2O_2-based HZO films with various number of oxidant pulses per cycle. For H_2O-based films, 7 pulses and 20 pulses were additionally examined to confirm the trend of crystallinity evolution.

Figure 3 showed the change of O/T/C phases peak area as a function of the number of oxidant pulses per cycle for both oxidants. It can be observed that both H_2O_2- and H_2O-based HZO films showed crystallization of O/T/C phases in the as-grown state, while H_2O_2-based films consistently resulted in a larger peak area than H_2O-based films. With increasing oxidant pulse numbers, those films exhibited clearly different crystallization behaviors. For the H_2O_2 case, the O/T/C phases peak area increased rapidly and reached saturation with five pulses, then remained at a similar level with further extension of oxidant exposure time. For the H_2O case, the crystallinity showed little change when the oxidant exposure was insufficient (≤7 pulses). Only when longer

exposure time was provided (≥10 pulses) did the peak area begin to increase, finally approaching saturation with 15 pulses. Notably, under sufficient oxidant exposure time, the O/T/C phases peak area of H_2O_2-based films remained ~30% higher than that of H_2O-based films, indicating an oxidant-dependent effect beyond simple dose limitation. The pulse-pressure and deposition-time artifacts on the film crystallinity associated with the higher N_2 carrier flow of Peroxidizer can be excluded, since the crystallinity showed no measurable change even if H_2O was supplied with similarly high pulse pressure with sufficient exposure time (data not shown).

C. Impurity evaluations

As shown in FIG. 3, the crystallinity difference between H_2O_2- and H_2O-based HZO films becomes significant after 5 oxidant pulses per cycle, and their crystallinities were both saturated at different levels at 15 pulses. As a result, to further investigate the factors causing this difference in the crystallinity of as-grown films, impurity concentrations were evaluated by SIMS for these four representative HZO films grown with 5 or 15 pulses with H_2O_2 or H_2O. A 10-nm-thick Al_2O_3 layer (Al_2O_3 cap.) was deposited on these films as a capping layer for SIMS measurement, to avoid the influence of surface-induced instable signals. Here, carbon and nitrogen were considered as the main impurities in the films[18]. The depth profiles of carbon and nitrogen in the films are shown in FIG. 4(a) and 4(b), respectively. The presence of carbon and nitrogen, consistent with the precursor ligand composition, suggests that these impurities predominantly arise from residual ligand fragments remaining after incomplete ligand-exchange reactions.

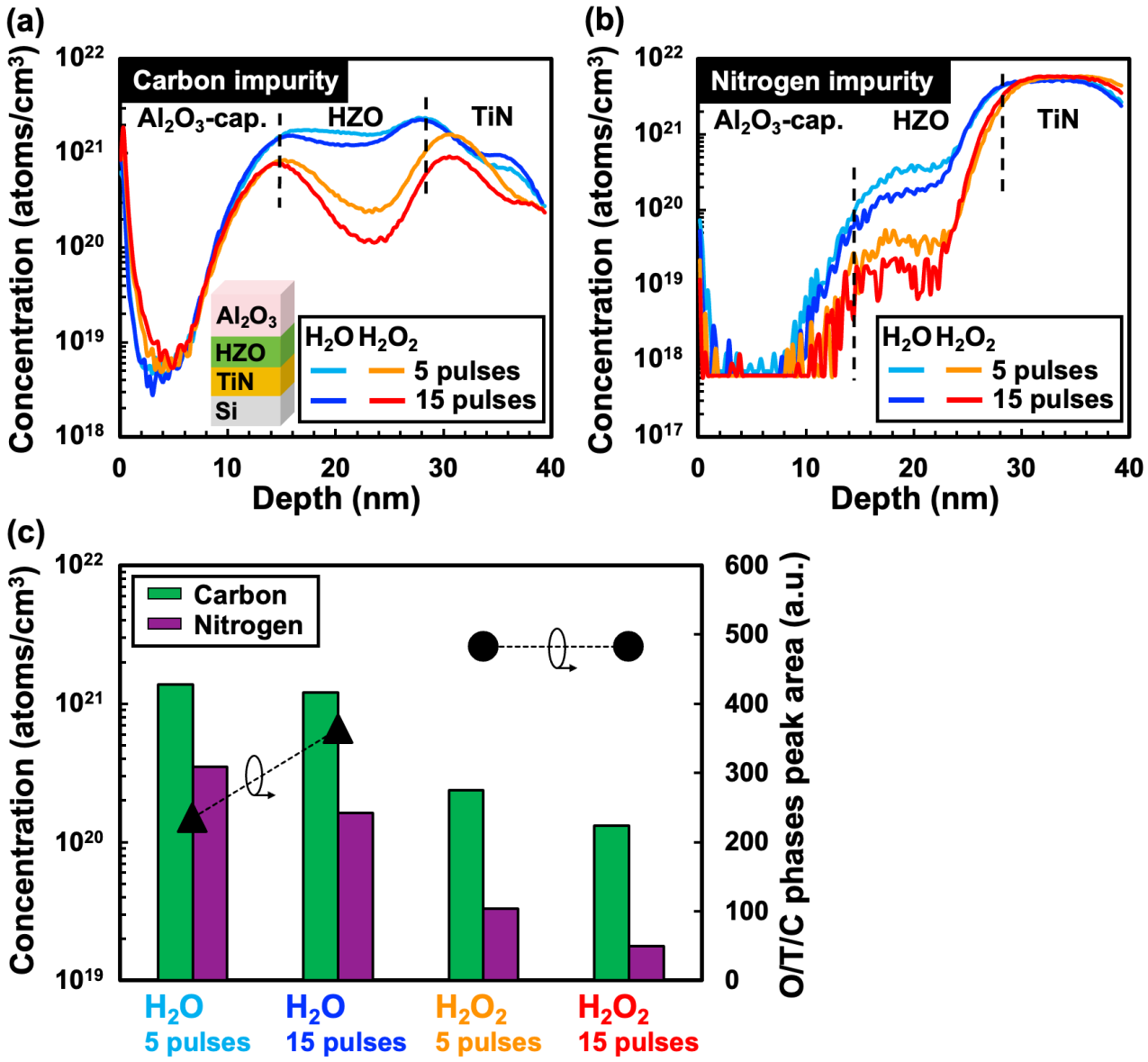

FIG. 4. SIMS depth profile of H_2O- and H_2O_2-based HZO films using 5 and 15 pulses per cycle: (a) carbon and (b) nitrogen. (c) Comparison of impurity concentrations of carbon and nitrogen and O/T/C phases peak area for H_2O- and H_2O_2-based HZO films deposited with 5 and 15 oxidant pulses per cycle. Bars (left y-axis) show the impurity concentrations, while the markers (right y-axis) show the O/T/C phases peak area, where triangles and circles represent the H_2O- and H_2O_2-based films, respectively.

It is also clear that increasing the number of oxidant pulses reduces the carbon and nitrogen concentrations in both H_2O- and H_2O_2-based films. It should be noted that impurities concentrations in the H_2O_2-based films are approximately one order of magnitude lower than those in the H_2O-based films even using excessive oxidation as 15 pulses per cycle, which clearly show a significantly higher efficiency of H_2O_2 for impurity removal. Carbon and nitrogen originated from residual ligands fragments can be reduced by oxidation, so this lower impurity level of H_2O_2-based films should be attributed to the higher oxidizing ability of H_2O_2. Figure 4(c) showed the comparison of impurity concentrations of carbon and nitrogen and O/T/C phases peak area for H_2O- and H_2O_2-based HZO films deposited with 5 and 15 oxidant pulses per cycle. For the H_2O-based films, the O/T/C phases peak area increased with decreasing impurity concentrations of both carbon and nitrogen by increasing number of oxidant pulses. Moreover, the H_2O_2-based films showed lower impurity concentrations of carbon and nitrogen compared to those of H_2O-based films, resulting in increase of the O/T/C phases peak area. This trend is consistent with previous reports, suggesting that carbon- and nitrogen-related residues may affect crystallization by hindering atomic migration[21] and by altering the local coordination environment[23], respectively. Since carbon and nitrogen decrease with a similar trend, the crystallinity change cannot be attributed to a single impurity species; instead, the data support that crystallinity generally increases with decreasing overall impurity level. For the H_2O_2-based films, on the other hand, O/T/C phases peak area exhibits saturation behavior even though impurities continue to decrease, suggesting that crystallization is not only affected by impurity concentration but also other factors. Once oxidation becomes sufficient, further impurity reduction can

have a diminished impact because additional crystallization would require further atomic rearrangement and microstructural evolution, which are kinetically constrained at the deposition temperature of 250 °C. Therefore, in the saturation region, crystallinity becomes less sensitive to impurity changes under the present deposition conditions.

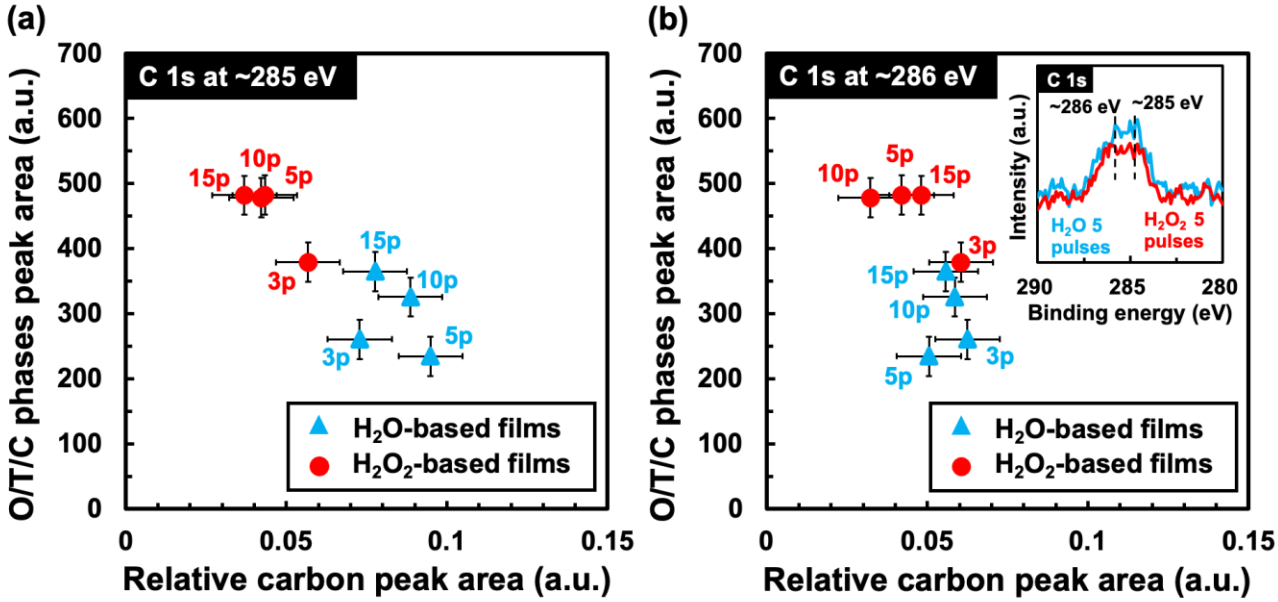

FIG. 5. Relationship between the O/T/C phases peak area and the relative peak area of C 1s at (a) ~285 and (b) ~286 eV for H_2O- and H_2O_2-based HZO films. Sample labels indicate oxidant type and pulse number, "p" denotes the number of oxidant pulses per cycle (e.g., 5p = 5 pulses per cycle). The inset shows representative XPS C 1s spectra for H_2O- and H_2O_2-based films with 5 oxidant pulses per cycle.

Because carbon and nitrogen showed similar concentration changing trends in representative SIMS profiles, C 1s core level spectrum was used as a practical indicator for systematic XPS analysis of impurity levels across HZO films grown using H_2O_2 or H_2O with 3, 5, 10, and 15 oxidant pulses per cycle. There were two peaks in C 1s XPS for all the films as shown in the inset of FIG. 5: the peak at ~285 eV assigned to C–C or

C–H bonds and the one at ~286 eV assigned to C–O or C–N bonds[32]. The relative carbon peak areas were calculated based on the ratio of C 1s/(Hf 4f + Zr 3d) signal. As shown in FIG. 5, the decrease in the peak area of ~285 eV component is associated with an increase in the O/T/C phases peak area for both oxidants (FIG. 5(a)), suggesting that this species might act as a crystallization retarder, whereas the peak area of ~286 eV component does not show a clear correlation with crystallinity (FIG. 5(b)). Even though a certain carbon-related species was suggested to affect the crystallinity, the possibility should be considered that nitrogen may play a more important role in determination of the crystallinity, which should be verified in future studies.

IV. SUMMARY AND CONCLUSIONS

The impurity concentration in as-grown HZO films decreases as the number of oxidant pulses per cycle increases, and the crystallinity generally increases as the impurity level is reduced, indicating that impurity reduction is an important factor for promoting crystallization of as-grown HZO films. Compared with H_2O, using H_2O_2 as the ALD oxidant results in higher crystallinity of as-grown HZO films, which is consistent with H_2O_2's superior oxidizing ability to remove impurities from the film during the ALD process. The saturation of crystallinity, despite a continued decrease in impurity concentration under sufficiently oxidizing conditions, suggests that crystallization is not affected by impurity level alone and may also be constrained by other factors such as process temperature.

ACKNOWLEDGMENTS

This study was partially supported by JSPS KAKENHI (No. JP24K17304 and No. JP24K21616) and MEXT Leading Initiative for Excellent Young Researchers (No. JPMXS0320220213).

AUTHOR DECLARATIONS

Conflicts of Interest *(required)*

The authors have no conflicts to disclose.

DATA AVAILABILITY

Data available on request from the authors.

REFERENCES

[1]T. S. Böscke, J. Müller, D. Bräuhaus, U. Schröder, and U. Böttger, Appl. Phys. Lett. **99**, 102903 (2011).

[2]Z. Gao, Y. Luo, S. Lyu, Y. Cheng, Y. Zheng, Q. Zhong, W. Zhang, and H. Lyu, IEEE Electron Device Lett. **42**, 1303 (2021).

[3]T. D. Huan, V. Sharma, G. A. Rossetti, and R. Ramprasad, Phys. Rev. B **90**, 064111 (2014).

[4]U. Schroeder, M. H. Park, T. Mikolajick, and C. S. Hwang, Nat. Rev. Mater. **7**, 653 (2022).

[5]X. Sang, E. D. Grimley, T. Schenk, U. Schroeder, and J. M. LeBeau, Appl. Phys. Lett. **106**, 162905 (2015).

[6]S. Mueller, J. Mueller, A. Singh, S. Riedel, J. Sundqvist, U. Schroeder, and T. Mikolajick, Adv. Funct. Mater. **22**, 2412 (2012).

[7]P. D. Lomenzo, Q. Takmeel, S. Moghaddam, and T. Nishida, Thin Solid Films **615**, 139 (2016).

[8]L. Alrifai, E. V. Skopin, N. Guillaume, P. Gonon, A. Bsiesy, Appl. Phys. Lett. **123**, 032901 (2023).

[9]S. J. Kim, Y. C. Jung, J. Mohan, H. J. Kim, S. M. Rho, M. S. Kim, J. G. Yoo, H. R. Park, H. Hernandez-Arriaga, J.-H. Kim, H. T. Kim, D. H. Choi, J. Jung, S. M. Hwang, H. S. Kim, H. J. Kim, and J. Kim, Appl. Phys. Lett. **119**, 242901 (2021).

[10]R. Alcalá, C. Richter, M. Materano, P. D. Lomenzo, C. Zhou, J. L. Jones, T. Mikolajick, and U. Schroeder, J. Phys. D: Appl. Phys. **54**, 035102 (2021).

[11]V. Mukundan, S. Consiglio, D. H. Triyoso, K. Tapily, M. E. McBriarty, S. Schujman, K. Beckmann, J. Hazra, V. Kaushik, N. Cady, R. D. Clark, G. J. Leusink, and A. C. Diebold, Phys. Status Solidi A **218**, 2100024 (2021).

[12]M. Materano, C. Richter, T. Mikolajick, and U. Schroeder, J. Vac. Sci. Technol. A **38**, 022402 (2020).

[13]B. S. Kim, S. D. Hyun, T. Moon, K. D. Kim, Y. H. Lee, H. W. Park, Y. B. Lee, J. Roh, B. Y. Kim, H. H. Kim, M. H. Park, and C. S. Hwang, Nanoscale Res. Lett. **15**, 72 (2020).

[14]J. Niinistö, M. Mäntymäki, K. Kukli, L. Costelle, E. Puukilainen, M. Ritala, M. Leskelä, J. Cryst. Growth **312**, 245 (2010).

[15]J.-H. Kim, T. Onaya, H. R. Park, Y. C. Jung, D. N. Le, M. Lee, H. Hernandez-Arriaga, Y. Zhang, E. H. R. Tsai, C.-Y. Nam, T. Nabatame, S. J. Kim and J. Kim, J. ACS Appl. Electron. Mater. **5**, 4726 (2023).

[16]W. C. Lee, C. J. Cho, S. Kim, E. S. Larsen, J. H. Yum, C. W. Bielawski, C. S. Hwang, and S. K. Kim, J. Phys. Chem. C **121**, 17498 (2017).

[17]M. Cho, D. S. Jeong, J. Park, H. B. Park, S. W. Lee, T. J. Park, C. S. Hwang, G. H. Jang, and J. Jeong, Appl. Phys. Lett. **85**, 5953 (2004).

[18]Y. K. Choi, K. Holsgrove, A. Watson, B. L. Aronson, M. K. Lenox, L. Shvilberg, C. Zhou, S. S. Fields, S. Wang, S. J. McDonnell, A. Kumar, and J. F. Ihlefeld, ACS Omega **10**, 20524 (2025).

[19]H.-S. Jung, H. K. Kim, I.-H. Yu, S. Y. Lee, J. Lee, J. Park, J. H. Jang, S.-H. Jeon, Y. J. Chung, D.-Y. Cho, N.-I. Lee, T. J. Park, J.-H. Choi, and C. S. Hwang, J. Electrochem. Soc. **159**, G33 (2012).

[20]Q. Xie, J. Musschoot, D. Deduytsche, R. L. Van Meirhaeghe, C. Detavernier, S. Van den Berghe, Y.-L. Jiang, G.-P. Ru, B.-Z. Li, and X.-P. Qu, J. Electrochem. Soc. **155**, H688 (2008).

[21]H.-S. Jung, S. H. Jeon, H. K. Kim, I.-H. Yu, S. Y. Lee, J. Lee, Y. J. Chung, D.-Y. Cho, N.-I. Lee, T. J. Park, J.-H. Choi, S. Han, and C. S. Hwang, ECS J. Solid State Sci. Technol. **1**, N33 (2012).

[22]G. He, Q. Fang, G. H. Li, J. P. Zhang, and L. D. Zhang, Appl. Surf. Sci. **253**, 8483 (2007).

[23]G. Shang, P. W. Peacock, and J. Robertson, Appl. Phys. Lett. **84**, 106 (2004).

[24]F. Rezaei, P. Vanraes, A. Nikiforov, R. Morent, and N. De Geyter, Materials **12**, 2751 (2019).

[25]Y. C. Jung, J.-H. Kim, H. Hernandez-Arriaga, J. Mohan, S. M. Hwang, D. N. Le, A. Sahota, H. S. Kim, K. Kim, R. Choi, C.-Y. Nam, D. Alvarez, J. Spiegelman, S. J. Kim, and J. Kim, Appl. Phys. Lett. **121**, 222901 (2022).

[26]T. Onaya, T. Nabatame, N. Sawamoto, A. Ohi, N. Ikeda, T. Nagata, and A. Ogura, Microelectron. Eng. **215**, 111013 (2019).

[27]T. Onaya, T. Nabatame, Y. C. Jung, H. Hernandez-Arriaga, J. Mohan, H. S. Kim, N. Sawamoto, C.-Y. Nam, E. H. R. Tsai, T. Nagata, J. Kim, and A. Ogura, APL Mater. **9**, 031111 (2021).

[28]M.-J. Choi, H.-H. Park, D. S. Jeong, J. H. Kim, J.-S. Kim, and S. K. Kim, Appl. Surf. Sci. **301**, 451 (2014).

[29]J.-H. Kim, S. Song, D. M. Narayan, D. N. Le, T. T. H. Chu, M. Lee, G. Park, S. Lee, J. Kang, J. Spiegelman, M. Benham, S. J. Kim, R. Choi, and J. Kim, Appl. Surf. Sci. **686**, 162197 (2025).

[30] L. Xu, T. Nishimura, S. Shibayama, T. Yajima, S. Migita, and A. Toriumi, J. Appl. Phys. **122**, 124104 (2017).

[31]T. Onaya, T. Nabatame, N. Sawamoto, A. Ohi, N. Ikeda, T. Nagata, and A. Ogura, APL Mater. **7**, 061107 (2019).

[32]T. R. Gengenbach, G. H. Major, M. R. Linford, and C. D. Easton, J. Vac. Sci. Technol. A **39**, 013204 (2021).